Consequences of Strong Vertical Accelerations on Shear Demand and Capacity in Bridge Columns

H. Lee, M.S. Günay and K.M. Mosalam
University of California, Berkeley, CA, USA

S.K. Kunnath
University of California, Davis, CA, USA

SUMMARY:
Strong vertical ground motions can significantly alter axial forces in a bridge column. Axial force variations also affect the concrete contribution to the shear capacity of a reinforced concrete (RC) member. However, the effect of axial force demands on shear capacity is a fairly complex issue since the shear demand in an RC bridge column is affected by variations in the axial force. A combined experimental and numerical study was carried out in a joint project between the University of California at Berkeley and Davis to examine the effects of vertical ground motions on the shear demand and shear capacity in columns of ordinary highway bridges. The experimental study consisted of a series of shaking table simulations on quarter-scale specimens. Results of the tests indicate that tension in the columns results in degradation of shear strength, which is mainly due to the degradation of the concrete contribution to shear strength.

Keywords: Bridge columns, shear capacity, shear demand, vertical ground motions.

1. INTRODUCTION

The consideration of vertical ground motions in the seismic design of highway bridges is gaining renewed interest because recent damaging earthquakes around the world have indicated the presence of significant vertical components in the recorded motions particularly close to the faults. Current provisions for the seismic design of bridges in California (SDC 2006) do not contain adequate guidelines on when and how to consider the adverse consequences of vertical accelerations in the design process. Past studies (Kunnath et al. 2008, Button et al. 2002, Collier and Elnashai 2001, Papazoglou and Elnashai 1996, Saadeghvaziri and Foutch 1991) have identified numerous issues resulting from axial force variations in bridge columns as a result of strong vertical accelerations. In addition to numerical studies, there have also been some limited experimental studies on the effect of vertical ground motions on reinforced concrete (RC) columns (Sakai and Unjoh 2007, Kim and Elnashai 2008).

Some of the issues already identified in previous research are further complicated by the fact that the frequency of vertical motion is higher than that of the horizontal motion. Hence, it is necessary to gain additional insight into high frequency axial variations on shear demand and shear capacity of typical bridge columns that are vulnerable to vertical effects of strong ground shaking.

The objective of this study was to examine the effects of axial force variation in bridge columns due to strong vertical ground motions and the influence of these axial force fluctuations on shear strength degradation. Two quarter-scale specimens (SP1 and SP2) with different transverse reinforcement ratios were constructed and tested on the UC-Berkeley shaking table at Richmond Field Station. As a result of an extensive numerical investigation and preliminary fidelity tests, the 1994 Northridge earthquake acceleration recorded at the Pacoima Dam was selected as an input motion for the shaking table study. The chosen ground motion was applied to the test specimens at various intensity levels ranging from 5% to 125% of the actual recorded motion.

2. EXPERIMENTAL STUDY: DESIGN

After careful consideration of the shaking table capacity and its performance under multi-directional excitation, it was decided that the ideal bridge configuration for testing would be a single column bent with a circular cross-section. The Plumas-Arboga Bridge was selected as the prototype system. It is a two-bent, three-span RC bridge designed by Caltrans according to post-Northridge design practice. The total length of the bridge is 139 m, the spans connected to abutments are about 40.5 m each and the span between columns is approximately 58.0 m. The aspect ratio along the 'Bent center line' (weak axis) is 3.58 and that along the 'Bridge center line' (strong axis) is 5.37. Fig. 2.1 shows the column elevation and cross-section details. Note that the cross-section shape was altered to a circular section with circular hoops. Separate numerical studies were conducted to verify that the seismic demands are not significantly altered by the change in the cross-section, refer to (Lee 2011) for details. Table 2.1 compares the cross-section properties of the prototype and the two model specimens.

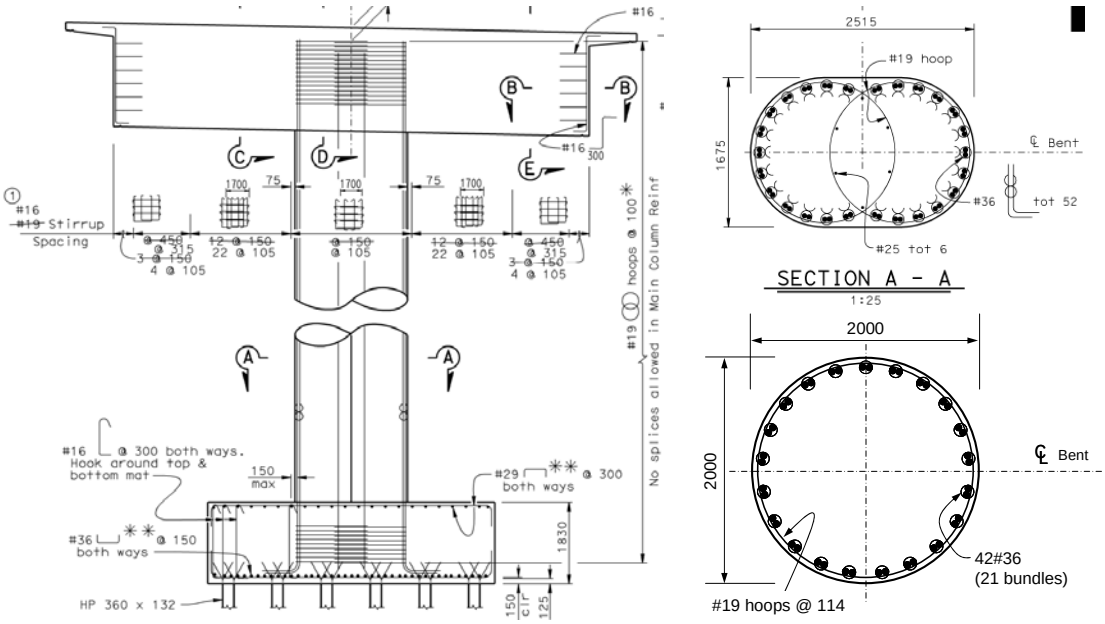

Figure 2.1. Prototype bridge column showing original and equivalent circular cross-sections (SI units).

Table 2.1. Cross-section properties (SI units).

Parameter	Unit	Prototype	SP1	SP2
Diameter, D	[m]	2.0	0.508	0.508
Area, A	[m^2]	3.14	0.203	0.203
Height, H	[m]	7.0	1.778	1.778
Longitudinal reinforcing bars		42#36	16#16	16#16
Diameter, d_{sl}	[mm]	35.8	15.875	15.875
Reinf. Ratio	[%]	1.348	1.563	1.563
Transverse reinforcing bars		#19@114	#6@51	#6@76
Diameter, d_{sh}	[mm]	19	6.35	6.35
Spacing, s	[mm]	114.3	50.8	76.2
Vol. Reinf. Ratio	[%]	0.543	0.545	0.363
$A_v D/s, A_v = 2A_{sh}$	[mm^2]	9929.2	623.4	415.6

The mass moment of inertia (MMI) is calculated as 64.0×10^3 kg-m^2 by scaling MMI of the prototype column using similitude relationships. MMI of the prototype column is determined such that the lateral period of the column matches the lateral period of the full-scale bridge system. A combination of concrete blocks, lead blocks, and steel beams on the test specimen provided the desired weight for the intended axial load ratio (ALR), height of C.G., and MMI. The target ALR was 6.5%, but the additional weight of steel beams and miscellaneous items caused slightly heavier gravity load on the column (6.8% ALR, i.e. about 85.6 kips). The test setup is shown in Fig. 2.2.

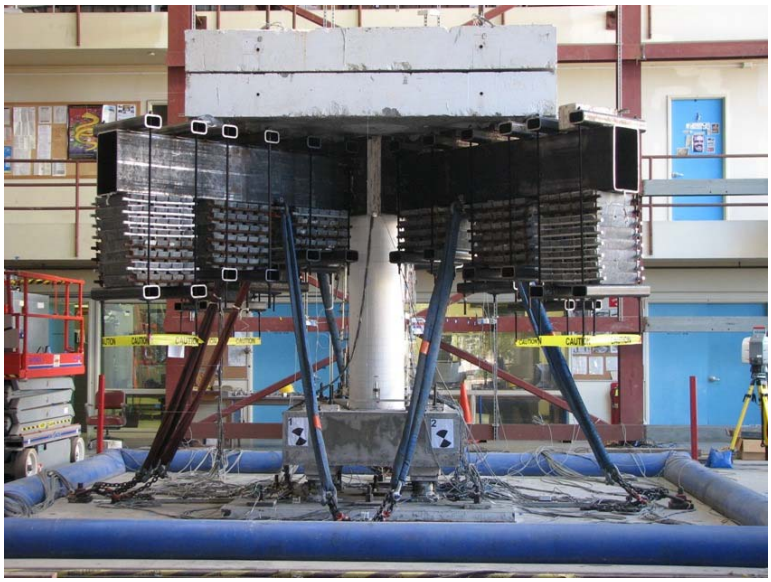

Figure 2.2. Final setup showing one of the model columns on the shaking table.

Total of 137 channels were used for each shaking table test consisting of 16 channels for monitoring accelerations and displacements of actuators under the table; 12 channels for tri-axial load cells monitoring restoring force of the specimen; 36 channels for accelerometers; 38 channels for strain gages on the longitudinal and transverse reinforcing bars; 35 channels monitoring local deformation and displacements of the test specimen. Additional details on the specimen designs, material properties and complete description of used instrumentation are reported in (Lee 2011).

3. EXPERIMENTAL STUDY: RESULTS

The ground motion recorded at the Pacoima Dam station of 1994 Northridge earthquake was applied to the two specimens. One of the horizontal (X) and the vertical (Z) components were utilized in most cases. Since the geometrical scale of the specimen corresponds to the ¼-scale model, each component of the ground motion was time-compressed by a factor of two as shown in Fig. 3.1. The acceleration time history in Fig. 3.1 is the unfiltered input ground motion obtained from the PEER NGA database. The ground motion was applied in increasing intensity levels varying in magnitude from 5% to 125%. Yielding of the specimens near the top of the column occurred when 50%-scale motion was applied. Even though the maximum curvature of SP1 was larger than that of SP2 during the 50%-scale run, this could be considered as the “yield-level” for both specimens. After this yield-level, 70%, 95%, and 125%-scale motions were applied.

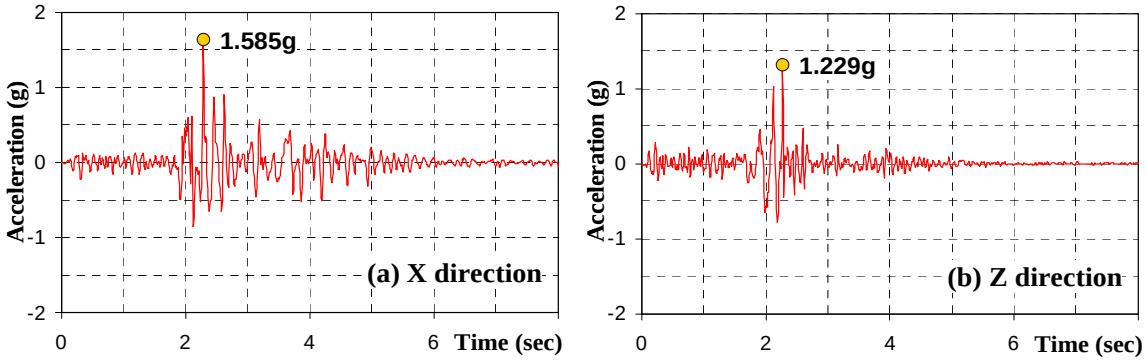

Figure 3.1. Horizontal (X) and vertical (Z) components of 100% Northridge earthquake.

Fig. 3.2 presents the time histories for the axial and shear forces obtained from the load cells for specimens SP1 and SP2 subjected to 125%-scale Northridge input and the corresponding runs are denoted as 1-9, 1-10, and 1-11 for SP1 and 2-9, 2-10, and 2-11 for SP2, respectively. For levels below the 125%-scale motion, the axial force did not induce tension in the column in most cases. SP2 with 95%-scale motion experienced very small peak axial tension of 1.4 kips. As the intensity increased, the peak-to-peak amplitude of the axial force increased significantly. Under 95%-scale motion, the axial force amplitude was almost twice as large as that under 50%-scale. However, the increase in the shear force was not as large as that in the axial force. The fact that the shear strength increase is less than that observed for the axial force is attributed to the fact that the shear forces at these intensities were no longer in the linear range, approaching the shear strength of the test specimens. As intended, the minimum axial force, i.e. minimum compression (positive) or maximum tension (negative), took place before the maximum shear force except for the cases of SP1 with the first 125%-scale motions.

Total of three 125%-scale tests were conducted for each specimen. The vertical component was not applied in the second of these three runs for each specimen (runs 1-10 and 2-10). Vertical acceleration was measured on the shaking table even if the vertical component was not applied because of the interaction of the vertical actuators which hold the vertical displacement at zero while balancing the forces due to the overturning moments caused by the horizontal acceleration. However, the axial force due to such inevitable vertical acceleration had relatively small compression values with limited effect on the RC column shear capacity. The peak axial and shear forces for the three runs with 125%-scale changed as follows: 252.8→144.5→208.4 kips (axial force) and 91.4→92.6→88.3 (shear force) for the respective runs 1-9→1-10→1-11 for specimen SP1 and 227.2→142.8→231.6 kips (axial force) and 77.4→80.9→77.2 kips (shear force) for the respective runs 2-9→2-10→2-11 for specimen SP2. For both specimens, the positive and negative shear force peaks change when the vertical component of ground motion is included, particularly the positive peak noticeably decreased after significant tension (57.9 kips for SP1 and 63.3 kips for SP2) in the column. The positive shear peak decreased from 92.6 kips to 80.5 kips in SP1 and from 80.9 kips to 67.0 kips in SP2. Considering that the shear forces were similar prior to significant tension for the "horizontal only" run, where for SP1, this force was 91.4 kips for run 1-9 and 92.6 kips for run 1-10 and for SP2, it was 77.4 kips for run 2-9 and 80.9 kips for run 2-10, the decrease of the positive peak shear force can be explained partly as a result of the vertical excitation, causing axial tension in the column. The reduction in shear force can be attributed to the reduction in the contribution of the concrete to the shear force capacity.

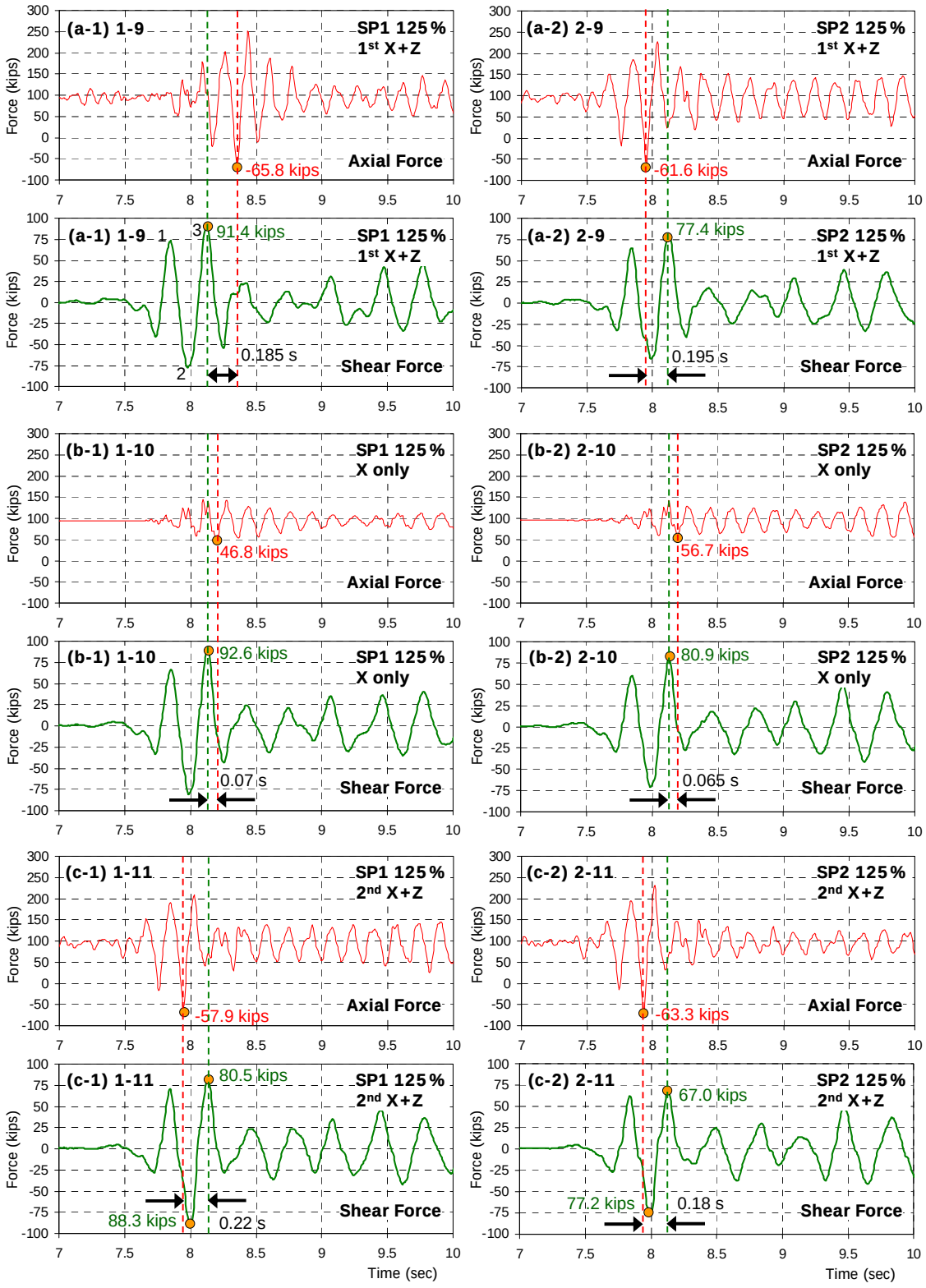

Figure 3.2. Axial force and shear force time histories for 125%-scale tests for both specimens (1 kip = 4.448 kN).

Considering the three 125%-scale tests together as a continuous test, it can be speculated that the reduction in the shear peak was due to degradation caused by the occurrence of two successive large axial tensile force peaks. Hence, the positive peak shear force reduced after the second axial tensile peak for both specimens. On the other hand, the peak axial tensile force in the "2nd horizontal + vertical" tests (runs 1-11 and 2-11) did not affect the negative peak shear force (88.3 kips in SP1 and 77.2 kips in SP2). This can be explained by crack opening and closing. Considering crack patterns observed after the 95%-scale, the 125%-scale "1st horizontal + vertical" and "horizontal only" tests, the diagonal cracks were concentrated near the top of the column, and the main direction was from south to north downwards, as shown in Fig. 3.3. Consequently, the opening of the diagonal cracks was caused by mass rotation and lateral displacement at the top at the first shear peak (Fig. 3.3a). On the contrary, the directions of rotation and translation at the second shear peak, i.e. the negative shear peak, resulted in closing of main diagonal cracks (Figure 3.3b). Even if tension occurred at the same time, its effect on crack opening would be minimal. Similar to the first peak, the crack opening occurred again at the third shear peak, i.e. the positive shear peak (Figure 3.3c), where the lateral displacement was almost twice as large as that at the first shear peak, in most of the 125%-scale tests. Therefore, the crack opening became more severe. It is to be noted that micro-cracks produced by tensile axial forces contribute to further widening of the diagonal cracks. This explanation stresses that micro-models may be necessary in certain cases to simulate the shear strength behavior under the combined effect of vertical and horizontal excitations.

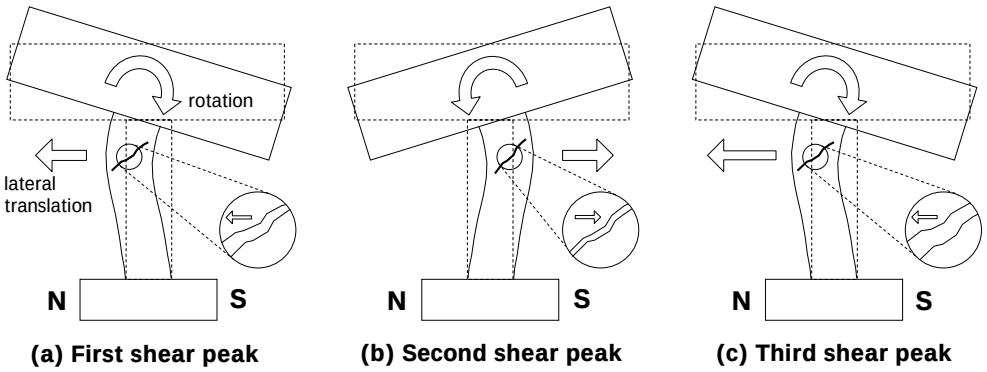

Figure 3.3. Shear crack opening and closing at each shear peak during the 125%-scale tests.

4. SHEAR STRENGTH DEMAND VERSUS SHEAR CAPACITY

In this section, the shear demands imposed by the applied ground motions on the two models SP1 and SP2 are compared with the available capacity estimates. Given the lack of more reliable or accurate methods to estimate the shear capacity of a RC section, the available shear strengths are estimated using ACI-318 (2008) and the provision of the California Department of Transportation Seismic Design Criteria (SDC 2010). The shear strength expression used in ACI is well-known and not repeated here. The SDC expression for shear strength of a RC column is given by:

$$V_n = V_c + V_s \tag{4.1}$$

$$V_s = \frac{A_v f_y D'}{s} \tag{4.2}$$

$$V_c = \nu_c A_e \tag{4.3}$$

In the above expressions, A_v is the cross-sectional area of the spiral reinforcement within spacing *s*,

f_y is the yield strength of the spiral reinforcement $A_e = 0.8A_g$ is the effective shear area and ν_c is determined by the location of the cross-section, transverse reinforcement, and ductility demand ratio.

Inside the plastic hinge zone,

$$\nu_c = \text{Factor1} \times \text{Factor2} \times \sqrt{f_c'} \le 0.33\sqrt{f_c'} \tag{4.4}$$

Outside the plastic hinge zone,

$$\nu_c = 0.25 \times \text{Factor2} \times \sqrt{f_c'} \le 0.33\sqrt{f_c'} \tag{4.5}$$

It should be noted that f_c' is the concrete strength in MPa. The factors in the above equations are defined as follows:

$$0.025 \le \text{Factor1} = \frac{\rho_s f_{yh}}{12.5} + 0.305 - 0.083\mu_d \le 0.25 \tag{4.6}$$

where f_{yh} is the transverse reinforcement (e.g. hoop) yield strength in MPa and $\rho_s f_{yh}$, where ρ_s is the volumetric ratio of the transverse reinforcement, is limited to 2.413 MPa.

$$\text{Factor2} = 1 + \frac{P_c}{13.8A_g} < 1.5 \tag{4.7}$$

where P_c is the axial load in N and A_g is in mm^2. It should be highlighted that $\nu_c = 0$ for members whose net axial load is in tension.

Although shear strength expressions from ACI and SDC were used in this study, it is important to highlight the fact that these expressions were developed to consider shear capacity under sustained compression or tension rather than the rapid axial force fluctuations induced by high frequency vertical motions. Hence, the objective in presenting the shear demand versus capacity plots is not necessarily to point to the deficiency in current codes but primarily to highlight the need to consider the effects of vertical excitation on axial force variations.

Fig. 4.1 compares the shear strength estimation of ACI and SDC equations with the absolute value of the shear force demand histories obtained from the test results. It should be noted that the axial forces and displacements obtained from the test results were used in these shear strength estimations. The two code equations provided similar estimations under compression, but they differed under tension. Since there was significant axial tension in run 1-11 for SP1 and run 2-11 for SP2, the SDC estimate reduced to V_s (shear strength provided by the hoops) only, i.e. 43.8 kips (194.8 kN) for SP1 and 27.5 kips (122.3 kN) for SP2, which correspond to 57.3% and 66.8% reduction compared to the initial full shear capacity, i.e. V_s+V_c where V_c is the shear strength provided by the concrete with no axial tension. Moreover, there were noticeable decreases in the SDC estimations due to large ductility demands. As a result, SDC equation provided a more conservative estimation than that of the ACI equation. Accordingly, the shear demands of SP1 and SP2 exceeded the shear capacity estimated by SDC in all the 125%-scale tests, consistent with the observed shear damage to the test specimens. However, the shear capacity estimates were overly conservative. The SDC shear capacity prediction was sometimes smaller than half of the shear force demand. Noting that the shear forces were obtained from the test data, therefore would need to be bounded by the shear capacity values, significant underestimation of the shear strength by the SDC equation can be witnessed. Finally, it was observed that the shear demand was consistently less than the shear strength estimation of ACI equation. Therefore, the ACI equation does not capture the observed shear damage.

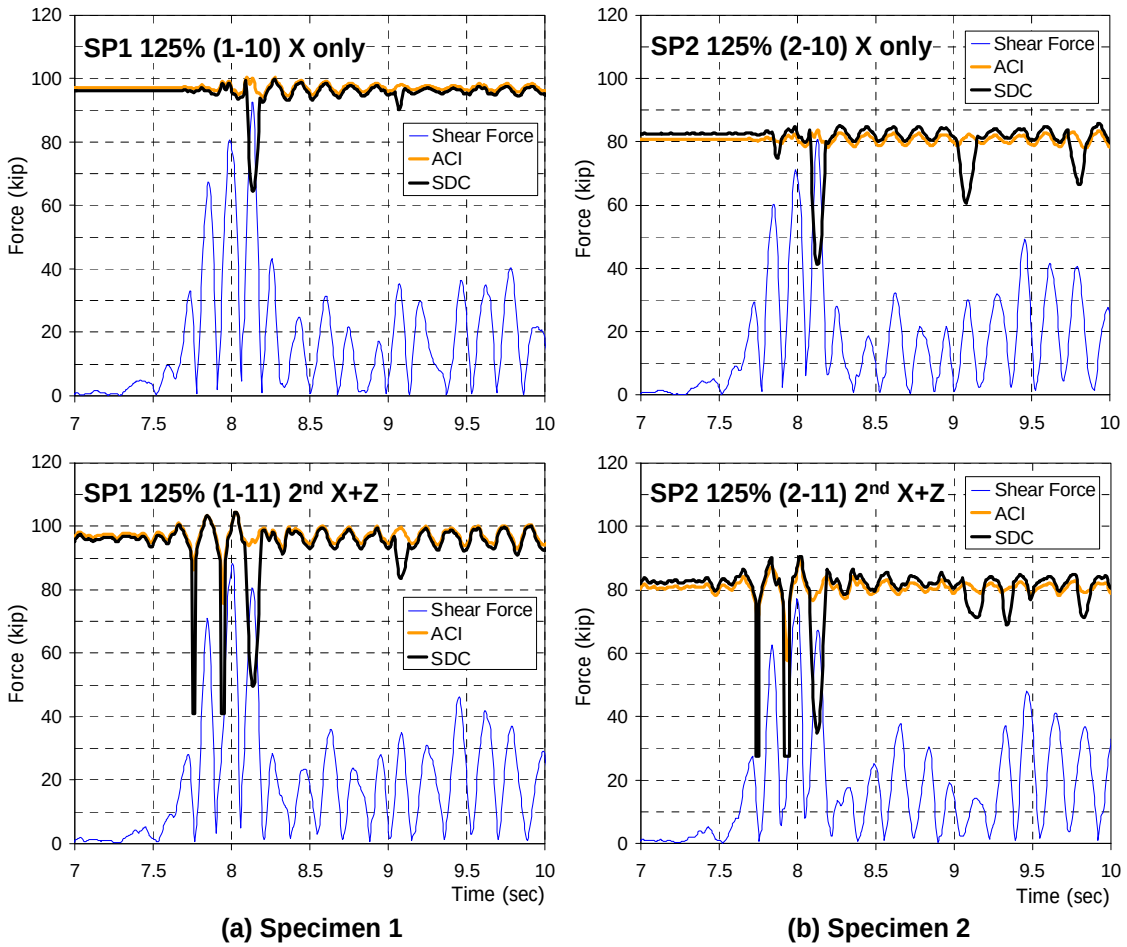

Figure 4.1. Comparison of shear force demand versus shear strength using ACI and SDC shear strength expressions for the 125%-scale tests (1 kip = 4.448 kN).

5. SUMMARY OF FINDINGS AND CONCLUDING REMARKS

Some of the main findings from the experimental phase of the study are summarized below:

- Flexural damage at the top of the columns took place before the flexural damage at the base since the bending moment at the top was larger. This was a result of the large mass moment of inertia at the top of the column. Reduction of the acceleration on the mass block due to the rotations contributed to this situation as well.
- As a result of flexural yielding at the top and base of the columns bending in double curvature, the induced shear force demand on the columns attained the shear capacity which would not have been the case if yielding occurred only at the base and the bending moment at the top was smaller than the yielding bending moment. Significant shear cracking was observed as a result of this situation.
- Considerable tensile force was induced on the test columns due to vertical excitation that resulted in degradation of shear strength, which was mainly due to the degradation of the concrete contribution to shear strength.
- Shear strength expressions of ACI and SDC were insufficient in predicting the observed shear damage. This was mostly attributed to the fact that these equations were developed to consider shear capacity under sustained compression or tension rather than the rapid axial force

fluctuations induced by high frequency vertical motions. Therefore, it was clear that there is a need for more accurate shear strength calculation methods under vertical excitations. Micro-models can be useful in certain situations to simulate the shear strength behavior under the combined effect of vertical and horizontal excitations.

ACKNOWLEDGEMENTS

Funding for this study provided by the California Department of Transportation (Caltrans) under Contract No. 59A0688 is gratefully acknowledged. Input and comments from Li-Hong Sheng, Mark Yashinsky, Mark Mahan and Fadel Alameddine are sincerely appreciated. The Pacific Earthquake Engineering Research (PEER) Center staff assistances, especially those of Mr. Wesley Neighbour, Mr. Nathaniel Knight, and Mr. David Maclam, were essential for the experimental study.

REFERENCES

ACI-318 (2008), Building Code Requirements for Structural Concrete and Commentary, ACI 318-08, American Concrete Institute, Farmington Hills, MI.

Button, M.R., Cronin, C.J. and Mayes, R.L. (2002). Effect of Vertical Motions on Seismic Response of Bridges. *ASCE Journal of Structural Engineering*, **128**:12, 1551-1564.

Collier, C.J. and Elnashai, A.S. (2001). A Procedure for Combining Vertical and Horizontal Seismic Action Effects. *Journal of Earthquake Engineering*, **5**:4, 521-539.

Kim, S. J. and Elnashai, A. S. (2008), "Seismic Assessment of RC Structures Considering Vertical Ground Motion," MAE Center report, No. 08-03.

Kunnath, S.K., Erduran, E., Chai, Y.H. and Yashinsky, M. (2008). Effect of Near-Fault Vertical Ground Motions on Seismic Response of Highway Overcrossings. *ASCE Journal of Bridge Engineering*, **13**:3, 282-290.

Lee, H. (2011). Experimental and Analytical Investigation of Reinforced Concrete Columns Subjected to Horizontal and Vertical Ground Motions. Ph.D. Dissertation, University of California, Berkeley.

Papazoglou, A.J. and Elnashai, A.S. (1996). Analytical and Field Evidence of the Damaging Effect of Vertical Earthquake Ground Motion. *Earthquake Engineering and Structural Dynamics*, **25**, 1109-1137.

Saadeghvaziri, M.A., and Foutch, D.A. (1991). Dynamic Behavior of R/C Highway Bridges under the Combined Effect of Vertical and Horizontal Earthquake Motions. *Earthquake Engineering and Structural Dynamics,* **20**, 535–549.

Sakai, J. and Unjoh, S. (2007), "Shake Table Experiment on Circular Reinforced Concrete Bridge Column under Multidirectional Seismic Excitation," Proceedings of the Research Frontiers, Structural Engineering Institute, American Society of Civil Engineers.

SDC (2010 "Seismic Design Criteria," California Department of Transportation (Caltrans) (2010), Sacramento, CA.